Spectroscopic analysis of 8-hydroxyquinoline derivatives and investigation of its reactive properties by DFT and molecular dynamics simulations

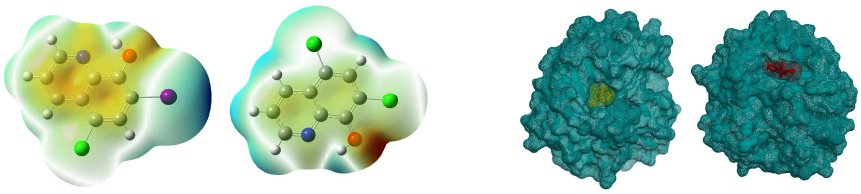

Spectroscopic analysis of 8-hydroxyquinoline derivatives and investigation of its reactive properties by DFT and molecular dynamics simulations

Sureshkumar.B[a], Sheena Mary.Y[b], K.S.Resmi[b], C.Yohannan Panicker[b*], Stevan Armaković[c], Sanja J. Armaković[d], C.Van Alsenoy[e], B.Narayana[f], Suma.S[a]

[a]Department of Chemistry, SN College, Kollam, Kerala, India

[b]Department of Physics, Fatima Mata National College, Kollam, Kerala, India

[c]University of Novi Sad, Faculty of Sciences, Department of Physics, Trg D. Obradovića 4, 21000 Novi Sad, Serbia

[d]University of Novi Sad, Faculty of Sciences, Department of Chemistry, Biochemistry and Environmental Protection, Trg D. Obradovića 3, 21000 Novi Sad, Serbia

[e]Department of Chemistry, University of Antwerp, Groenenborgerlaan 171, B-2020, Antwerp, Belgium

[f]Department of Chemistry, Mangalore University, Mangalagangothri, Mangaluru, Karnataka, India

*****author for correspondence:email: cyphyp@rediffmail.com

Abstract

Two 8-hydroxyquinoline derivatives, 5,7-dichloro-8-hydroxyquinoline (57DC8HQ) and 5-chloro-7-iodo-8-hydroxy quinoline (5CL7I8HQ) have been investigated in details by means of spectroscopic characterization and computational molecular modelling techniques. FT-IR and FT-Raman experimental spectroscopic approaches have been utilized in order to obtain detailed spectroscopic signatures of title compounds, while DFT calculations have been used in order to visualize and assign vibrations. The computed values of dipole moment, polarizability and hyperpolarizability indicate that the title molecules exhibit NLO properties. The evaluated HOMO and LUMO energies demonstrate the chemical stability of the molecules. NBO analysis is made to study the stability of the molecules arising from hyperconjugative interactions and charge delocalization. DFT calculations have been also used jointly with MD simulations in order to investigate in details global and local reactivity properties of title compounds. Also, molecular docking has been also used in order to investigate affinity of title compounds against decarboxylase inhibitor and quinoline derivatives can be a lead compounds for developing new antiparkinsonian drug.

Keywords: DFT; ALIE; RDF; BDE; Quinoline.

1. Introduction

Quinoline derivatives have wide applications such as optical switches in nonlinear optics, live saving drugs, sensors in electrochemistry and in the field of inorganic chemistry [1, 2]. Chloroquinoline derivatives exhibit antileishmanial activity [3] and antimalarial activity [4-7]. Hydroxyquinoline derivatives are commonly used for chelating metal cations and are highly fluorescent [8-11], and used for quantification of metal ions. Computational molecular modelling techniques, namely first principles calculations and MD simulations, are irreplaceable tools for evaluation of reactive properties of organic molecules similar to ones investigated in this study [12-16]. Finding appropriate approaches for removal and degradation of organic pharmaceutical molecules is one of the main tasks in front of the scientific community. Degradation procedures are being constantly improved thanks to the utilization of density functional theory (DFT) calculations and molecular dynamics (MD) simulations in order to predict the most important reactive parameters of molecules [17-20]. Oxidation mechanism and advanced oxidation processes are one the most important reaction mechanisms when it comes to the degradation procedures for removal of toxic organic pollutants and many aspects of these mechanisms can be addressed thanks to the computational molecular modelling techniques [21-23]. In this regard, DFT calculations have been used in this work in order to study sensitivity towards autoxidation mechanism, while MD simulations have been used in order to address the stability of title molecules in water.

2. Experimental details

Fine samples of the title compounds were obtained from Sigma Aldrich chemical company, USA and used without any further purification for spectral measurements. The FT-IR spectra (Fig.1) of the title compounds were recorded in the region 4000-400 cm^{-1} using Perkin-Elmer spectrum RX1 spectrometer equipped with Helium-Neon laser source, potassium bromide beam splitter and LiTaO3 detector. The sample was prepared by pressing the title compound with KBr into pellet form. The FT-Raman spectra (Fig.2) of the title compounds were recorded in 4000-0 cm^{-1} with a Nocolet model 950 FT-Raman spectrometer at 4 cm^{-1} spectral resolution using the 1064 nm line of a Nd:YAG laser for excitation at a 200 mW output power.

3. Computational details

Calculations of the wavenumbers, polarizability values, frontier molecular orbital analysis of the title compounds (Fig.3) were carried out with Gaussian 09 program [24] using the B3LYP/SDD quantum chemical calculation method. A scaling factor of 0.9613 is used to scale the theoretically obtained wavenumbers [25] and the assignments of the vibrational wavenumbers are done by using GaussView [26] and GAR2PED software [27]. Schrödinger Materials Science Suite 2017-3(SMSS) has been utilized for DFT calculations and MD

simulations of two 8-hydroxyquinoline derivatives. DFT calculations have been performed with Jaguar 9.6 [28] program and Desmond [29-32] program was used for MD simulations. B3LYP exchange-correlation functional [33] was used with 6-311++G(d,p), 6-31+G(d,p) and 6-311G(d,p) basis sets, for calculations of ALIE, Fukui functions and BDEs, respectively. OPLS3 force field [29, 34-36] was used for MD simulations. Simulation time was set to 10 ns, temperature to 300 K, pressure to1.0325 bar and cut off radius of 10 Å. Isothermal–isobaric (NPT) ensemble class was considered, while simple point charge (SPC) model [37] was used for the treatment of solvent. For MD simulations system was modelled by placing one molecule into the cubic box with approximately 2000 water molecules. All calculations and simulations by Jaguar and Desmond programs have been prepared and analyzed with Maestro GUI [38].

4. Results and disucssion

4.1 IR and Raman spectra

In the following discussion, the rings, C1-C2-C3-C4-C5-C6 and C4-C5-C10-C9-C8-N7 are designated as PhI and PhII and the observed IR, Raman bands, theoretical scaled wavenumbers and vibrational assignments are given in table 1.

The aromatic CH stretching modes in poly substituted benzenes [39] absorb between 3000 and 3120 cm^{-1} and for the title compounds, the bands at 3090 (PhI) and 3083, 3067, 3037 cm^{-1} (PhII) (DFT) are assigned the CH stretching vibrations of 57DC8HQ and 3119 cm^{-1} (PhI) and 3124, 3104, 3088 cm^{-1} (PhII) (DFT) for 5CL7I8HQ [40]. These modes are observed at 3082, 3035 cm^{-1} (57DC8HQ), 3085 cm^{-1} (5CL7I8HQ) in the IR spectrum and at 3070, 3033 cm^{-1} (57DC8HQ), 3127, 3099, 3074 cm^{-1} (5CL7I8HQ) in the Raman spectrum experimentally. Theoretically, the ring stretching modes of the phenyl rings are assigned at 1591, 1543,1432, 1385, 1368 cm^{-1} for PhI, 1570, 1543, 1467, 1348, 1315 cm^{-1} for PhII (57DC8HQ) and at 1593, 1536, 1423, 1390, 1304 cm^{-1} for PhI, 1561, 1536, 1458, 1351, 1304 cm^{-1} for PhII (5CL7I8HQ) [41]. These ring stretching modes of the title compounds, are observed experimentally at 1370 cm^{-1} (PhI), 1575, 1467, 1322 cm^{-1} (PhII) in the IR spectrum, 1601, 1540, 1388, 1371 cm^{-1} (PhI), 1569, 1540, 1465, 1344, 1318 cm^{-1} (PhII) in the Raman spectrum for 57DC8HQ and at 1602, 1393, 1315 cm^{-1} (PhI), 1565, 1458, 1315 cm^{-1} (PhII) in the IR spectrum, 1601, 1390, 1307 cm^{-1} (PhI), 1565, 1460, 1349, 1307 cm^{-1} (PhII) cm^{-1} in the Raman spectrum for 5CL7I8HQ. For poly substituted phenyl rings the ring breathing mode is reported at 1006 cm^{-1} (IR) and at 998 cm^{-1} (DFT) [42] and at 1003 cm^{-1} (DFT) [20]. DFT calculations give the ring breathing mode of poly substituted phenyl rings of 57DC8HQ at 1023 cm^{-1} and 5CL7I8HQ at 1016 cm^{-1}. The in plane CH bending vibrations are assigned at 1215 cm^{-1} (IR), 1215 cm^{-1} (Raman), 1212 cm^{-1} (DFT) for PhI,

1190, 1060 cm^{-1} (IR), 1128, 1070 cm^{-1} (Raman), 1188, 1121, 1067 cm^{-1} (DFT) for PhII (57DC8HQ) and at 1187 cm^{-1} (DFT) for PhI, 1125, 1049 cm^{-1} (IR), 1168, 1125, 1050 cm^{-1} (Raman), 1163, 1120, 1056 cm^{-1} (DFT) for PhII (5CL7I8HQ) as expected in literature [41]. The out-of-plane CH bending modes of the title compounds, are assigned at 957, 784 cm^{-1} (IR), 958, 928, 851, 770 cm^{-1} (Raman), 957, 925, 849, 782 cm^{-1} (DFT) for 57DC8HQ and at 954, 885, 835 cm^{-1} (IR), 949, 835 cm^{-1} (Raman), 1000, 952, 892, 833 cm^{-1} (DFT) for 5CL7I8HQ which are expected below1000 cm^{-1} according to literature [41].

According to literature [43] stretching modes of quinoline ring are reported at: 1563 cm^{-1} (IR), 1560 cm^{-1} (Raman) and 1568 cm^{-1} (DFT) (C=C stretching); 1500 cm^{-1} (Raman) and 1527 cm^{-1} (DFT) (C=N stretching); 1281 cm^{-1} (IR), 1285 cm^{-1} (Raman) and 1285 cm^{-1} (DFT) (C-N stretching); 1476 cm^{-1} (IR), 1205 cm^{-1} (Raman), 1204 and 1474 cm^{-1} (DFT) (C-C stretching). According to literature [41] the in-plane OH bending mode is expected in the range 1400-1480 cm^{-1} and the bands at 1388 cm^{-1} (Raman), 1385 cm^{-1} (DFT) and 1369 cm^{-1} (IR), 1365 cm^{-1} (DFT) are assigned as the OH in-plane deformation modes for 57DC8HQ and 5CL7I8HQ. The hydroxyl C-O stretching mode is assigned at 1245 cm^{-1} (DFT) for 57DC8HQ and 1237 cm^{-1} (DFT) for 5CL7I8HQ, which is expected in the range 1180-1260 cm^{-1} [44,45]. The out-of-plane OH deformation is assigned at 650 ± 80 cm^{-1} [41] and in the present case this mode is assigned at 592 cm^{-1} and 657 cm^{-1} (DFT) for 57DC8HQ and 5CL7I8HQ, respectively. In the present study, the CI stretching mode is assigned at 345 cm^{-1} and the reported values are 333 cm^{-1} [46] and 317 cm^{-1} [47]. For the title compound, 5CL7I8HQ, CCl stretching mode is assigned at 654 cm^{-1} and at 705, 653 cm^{-1} for 57DC8HQ as expected [48]. The reported values of C-Cl stretching modes are 670 cm^{-1} (IR), 663 cm^{-1} (Raman) and 665 cm^{-1} (DFT) [49].

4.2 Nonlinear optical properties

Nonlinear optics explains the interaction of electromagnetic fields in various materials to produce new electromagnetic fields, altered in wavenumber and other physical properties of the molecular systems [50,51]. The calculated polarizability of 57DC8HQ and 5CL7I8HQ are 2.146×10^{-23} and 2.067×10^{-23} esu. The dipole moments of 57DC8HQ and 5CL7I8HQ are respectively, 3.651 and 3.657 Debye. The fist order hyperpolarizabilities are 6.755×10^{-30} and 8.206×10^{-30} esu for 57DC8HQ and 5CL7I8HQ which are comparable with the reported values of similar derivatives [43] and these values are 51.96 and 63.12 times that of the standard NLO material urea [52]. The reported values of first hyperpolarizability of similar derivatives are 5.37×10^{-30} [43] and 16.9×10^{-30} [53]. The theoretically predicted second order hyperpolarizabilites are -6.461×10^{-37} esu for 57DC8HQ and -9.696×10^{-37} esu for 5CL7I8HQ and the reported values are -28.33×10^{-37} esu [43], -21.14×10^{-37} esu [54]. Hence the title

compounds and its derivatives are good objects for further studies of nonlinear optical properties. The calculated C-N distances (1.3164 to1.3771Å) in the molecular structures of the title compounds are in between a single and double bond length C-N bond and hence suggest an extended π-electron delocalization of the quinoline moiety, which were responsible for the nonlinearity of the molecules [55].

4.3 Frontier molecular orbital analysis

Visualization presented in Fig. 4 indicates the importance of iodine and chlorine atoms, as HOMO is practically completely delocalized in the near vicinity of these atoms. This result designates iodine and chlorine atoms to act as electron donor during the interactions with other molecules. HOMO is delocalized over the entire region of 57DC8HQ and except for the ring PhII of 5CL7I8HQ. On the other side LUMO orbital is mainly delocalized over the entire rings of 57DC8HQ and 5CL7I8HQ. Using information on the energies of HOMO and LUMO, useful and frequently used quantum-molecular descriptors such as the ionization energy and electron affinity can be calculated according to the following simple relations: $I = -E_{HOMO}$, $A = -E_{LUMO}$, $\eta = (-E_{HOMO} + E_{LUMO})/2$ and $\mu = (E_{HOMO} + E_{LUMO})/2$ [56]. Parr et al. [57] proposed the global electrophilicity power of a ligand as $\omega = \mu^2/2\eta$. For the title compounds, energy difference between HOMO and LUMO, HOMO-LUMO gap, are equal to 2.231 eV for 57DC8HQ and 0.80eV for 5CL7I8HQ. Ionization potential, I, and electron affinity, A, are calculated to be 7.347 eV, 5.116 eV and 5.891, 5.091eV for 57DC8HQ and 5CL7I8HQ, respectively. The values of HOMO-LUMO gap and global hardness (η = 1.116 for 57DC8HQ and 0.4eV for 5CL7I8HQ are almost the same as in the case of other similar derivatives that we have previously investigated [43, 54]. Although the stability parameters of these derivatives are practically the same, there are significant differences in the values of chemical potential and global electrophilicity. Also, the calculated electrophilicity of the 57DC8HQ and 5CL7I8HQ molecules are 17.40 and 94.22 eV, which is significantly lower than the value of electrophilicity of derivative in the work of Rajeev et al. [43,54], with the values of 28.29 and 24.40 eV, meaning that the title molecules are much more stable.

4.4 Molecular electrostatic potential maps

Molecular electrostatic potential (MEP) simultaneously displays molecular shape, size and electrostatic potential in terms of colour grading and provides a visual technique to comprehend the relative polarity of the molecule as shown in Fig.5 [58]. Different values of the electrostatic potential are represented by various colours; red < organge < yellow < green < blue. In the MEP maximum negative region represents the site for electrophilic attack indicated by red colour while the maximum positive region represents nucleophilic attack indicated by blue colour. From the MEP plot of the title compound it is clearly seen that

oxygen and ring groups are most electronegative region suitable for electrophilic attack and hydrogen atoms are most electropositive region suitable for nucleophilic attack.

4.5 ALIE surface, Fukui functions and noncovalent interactions

MEP surface is frequently used quantum-molecular descriptor for identification of electrophilic and nucleophilic molecular sites. However, clearer picture in terms of sensitivity towards electrophilic attacks can be obtained employing the concept of average local ionization energy (ALIE). ALIE descriptor represents the energy required for removal of an electron from molecule. ALIE values can be calculated according to the definition provided by Politzer and co-workers [59-63], while best visualization of this descriptor is achieved by mapping of its values to the electron density surface, which has been done in this work. Representative ALIE surfaces of 5CL7I8HQ and 57DC8HQ molecules have been provided in Fig.6. According to the ALIE surfaces it can be expected that 5CL7I8HQ molecule is much more sensitive towards the electrophilic attacks comparing to 57DC8HQ, due to the fact that it's minimal ALIE value is lower for almost 40 kcal/mol. The lowest ALIE values in case of the 5CL7I8HQ molecule are localized in the near vicinity of iodine atom, while in the case of 57DC8HQ molecule the lowest ALIE values are delocalized practically over the whole molecules. On the other side, concerning the highest ALIE values, both molecules are characterized by practically the same values, around 383 kcal/mol.

The concept of Fukui functions has been employed in this work beside MEP and ALIE surfaces, in order to identify possibly important reactive sites of molecules studied in this work. Fukui f^+ and f^- functions in Jaguar program are calculated in finite difference approximation, according to equations:

$$f^+ = \frac{\left(\rho^{N+\delta}(r) - \rho^N(r)\right)}{\delta}, \tag{1}$$

$$f^- = \frac{\left(\rho^{N-\delta}(r) - \rho^N(r)\right)}{\delta}, \tag{2}$$

where N stands for the number of electrons in reference state of the molecule, while δ stands for the fraction of electron which default value is set to be 0.01 [64]. For the sake of clearer visualization, the values of Fukui functions have been also mapped to the electron density surface (Fig.7), although they can be visualized with Maestro GUI as iso-surfaces as well. In order to interpret results concerning Fukui functions, it is necessary to identify positive colour (purple colour) in case of Fukui f^+ function and negative colour (red colour) in case of Fukui f^- function. Purple colour of Fukui f^+ function denotes areas where electron density increases after the addition of charge, while negative colour of Fukui f^- function denotes areas where electron density decreases after the removal of charge. Positive colour in case of the Fukui f^+

function of 5CL7I8HQ is clearly localized in the near vicinity of iodine atom, indicating that here electron density increased after the addition of charge. Therefore, this molecule site becomes electron rich part of the molecule during the reactions in which charge transfers to this molecule. Negative colour in case of the Fukui f^- function of the 5CL7I8HQ molecule is not particularly localized. On the other side, positive colour in the case of Fukui f^+ function in case of 57DC8HQ is localized at two specific spots around hydrogen atoms of pyridine ring. Comparing with 5CL7I8HQ molecule, it can be seen in case of 57DC8HQ that electron density increased to much lower extent, indicating much higher electrophilic character of 5CL7I8HQ.

4.6 Natural bond orbital analysis

The natural bond orbitals (NBO) calculations of the title compounds were performed using NBO 3.1 program [65-68] as implemented in the Gaussian09 package at the DFT/B3LYP level and the important results are presented in tables S1 and S2 (supporting materials).The stronger interactions are n_1C_5 with $\pi^*(C_9\text{-}C_{10})$, $\pi^*(C_6\text{-}C_1)$ and $n_2O_{11}\rightarrow\pi^*(C_2\text{-}C_3)$ having the energy values 58.36, 58.61 and 37.51 kJ/mol for 57DC8HQ and $n_1C_5\rightarrow\pi^*(C_6\text{-}C_1)$, $n_2O_{11}\rightarrow\pi^*(C_2\text{-}C_3)$ has the highest E(2) value 60.53, 33.80 kJ/mol for5CL7I8HQ.For the title compounds, 100% p-character was observed in lone pair of $n_2Cl_{12,}$ $n_3Cl_{12,}$ $n_2O_{11,}$ n_3Cl_{13} and π bonding of $C_9\text{-}C_{20,}$ $C_6\text{-}C_1$ and $C_2\text{-}C_3$ for 57DC8HQ and in π bonding of $C_9\text{-}C_{10}$,$C_1\text{-}C_6$,$C_2\text{-}C_3$ and the lone pairs of n_1C_5, $n_2Cl_{12,}$ $n_3Cl_{12,}$ n_2O_{11} and n_3I_{13} for 5CL7I8HQ.

4.7 Reactive and degradation properties based on autoxidation and hydrolysis

Since oxidative reactions are one of the most important reactions for the removal and degradation of toxic organic compounds [69], in this work we have decided to calculate bond dissociation energies (BDE) for hydrogen abstraction (H-BDE); a quantity which reflects the sensitivity of molecules towards the autoxidation mechanism [12]. H-BDE values and BDE values for the remaining single acyclic bonds have been summarized in Fig.8. H-BDE taking values between 70 and 85 kcal/mol [70, 71] reflects the significant sensitivity of molecules towards the autoxidation. H-BDE values between 85 and 90 kcal/mol also might indicate sensitivity towards the autoxidation [71]. Although it might be expected that H-BDE values lower than 70 kcal/mol indicate very high sensitivity towards autoxidation, this is however not the case [12, 70,72]. Results provided in Fig.8 indicate that both molecules might be stable towards the autoxidation mechanism, although H-BDE values for O-H bond for both molecules are relatively close to the upper border level of 90 kcal/mol. In Fig.8 it can be also noticed that BDE for iodine atom is much lower than BDE

for chlorine atom at the same position, indicating that 5CL7I8HQ molecule might be more prone to the degradation than 57DC8HQ.

The influence of water to the stability of organic molecules is also of great importance; especially when it is taken into account that majority of organic pharmaceutical molecules eventually end up in some type of the water. To address the stability of title molecules in water, we have performed MD simulations and calculated radial distribution functions (RDF) in order to identify atoms of these two 8-hydroxyquinoline derivatives with significant interactions with water molecules. RDFs of atoms with relatively significant interactions with water molecules have been presented in Fig.9. RDFs of atoms with significant interactions with water molecules for both molecules are pretty much similar. Certainly the most important interactions with water molecules have been identified for hydrogen atom of the OH group, with maximal g(*r*) value being located at distance somewhat lower than 2 Å. With respect to distance of the maximal g(*r*) value, hydrogen atom H18 is followed by the oxygen atom, with maximal g(*r*) value higher than 3 Å. Although chlorine and iodine atoms have relatively significant maximal g(r) values, they are located at distances higher than 3.5 Å. Since maximal g(*r*) value of iodine atom in 5CL7I8HQ molecule is slightly higher than maximal g(r) value of the corresponding chlorine atom in 57DC8HQ molecule, it can be stated that 5CL7I8HQ has just a little bit stronger interactions with water molecules.

4.8 Molecular docking

Parkinson's disease (PD) is the most frequent movement disorder and its burden on our society is expected to escalate, as the population ages. Specific factors causing selective death of nigral dopamine neurons, which lie at the root of Parkinson’s disease, are still unknown. Currently available treatments are symptomatic and, in many patients, eventually trigger severe side effects, such as dyskinesia. There is an urgent need to design new antiparkinsonian drugs and number of modified quinolines compounds show some promise in this regard. The anti-malarials containing the scaffold 4-amino-7-chloroquinoline is synthetic agonists used as neuro protective therapeutics for PD [73]. 1,2,3,4-Tetrahydroiso-Quinoline (TIQ) and its derivatives which are both endogenous and environmental substances is also used as chronic drug for PD [74].From the PASS (Prediction of Activity Spectra) [75] analysis of the quinolone derivatives and the predicted activities tabulated in the table 2 and the decarboxylase inhibitor with probability to be active (Pa) value around 0.9 and is used as a target for docking study. High resolution crystal structure of decarboxylase inhibitor was downloaded from the RSCB protein data bank website with PDB ID: 1KV8. Several author groups reported the therauptic effect of antiparkinson’s medication decarboxylase inhibitor [76, 77]. The molecular docking calculations were performed on Auto Dock-Vina software

[78-80]. The ligand binds at the active site of the substrate by weak non-covalent interactions and these interactions are depicted in Fig.10. The docked ligand forms a stable complex with decarboxylase inhibitor (Fig.11) and got a binding affinity value of -6.0 kcal/mol for 57DC8HQ and -5.1 kcal/mol for 5CL7I8HQ (Table 3). Thus the quinolone derivatives can be a lead compounds for developing new antiparkinsonian drug.

Conclusion

The FT-IR and FT-Raman spectra of the organic compounds, 5,7-dichloro-8-hydroxyquinoline and 5-chloro-7-iodo-8-hydroxy quinoline were recorded and analyzed.

The complete vibrational assignments of all the fundamental bands observed in FT-IR and FT-Raman spectra of the title molecules are made unambiguously using PED analysis. The dipole moment, polarizability, first order and second order hyperpolrizability values evaluated in the DFT calculations demonstrate that the title molecules may considered as the materials for NLO applications. MEP analysis gives the reactive regions in the molecules. ALIE surfaces indicate that 5CL7I8HQ molecule has much higher sensitivity towards electrophilic attacks, due to the fact that its minimal ALIE value is lower for 36 kcal/mol than in the case of 57DC8HQ molecule. Minimal ALIE value of the 5CL7I8HQ molecule is clearly localized in the near vicinity of iodine atom. Fukui functions also indicate the importance of iodine atom, since according to the Fukui f^+ function electron density significantly increased in it's vicinity, as a consequence of charge addition. H-BDE values indicate stability of both 5CL7I8HQ and 57DC8HQ molecules towards the autoxidation mechanism. RDFs indicate that in case of the both molecules, the most important interactions with water molecules occurred for the hydrogen atom H18. The docked title molecules form a stable complex with decarboxylase inhibitor and can be a lead compounds for developing new antiparkinsonian drug.

Acknowledgment

Part of this work has been performed thanks to the support received from Schrödinger Inc.
Part of this study was conducted within the projects supported by the Ministry of Education, Science and Technological Development of Serbia, grant numbers OI 171039 and TR 34019.

References

[1] S.A. Khan, A.M. Asiri, S.H. Al-Thaqafy, H.M.F. Aidallah, S.A. El-Daly, Synthesis, characterization and spectroscopic behavior of novel 2-oxo-1,4-disubstituted-1,2,5,6-tetrahydrobenzo[h]quinoline-3-carbonitrile dyes, Spectrochim. Acta 133 (2014) 141-148.

[2] C.B. Sangani, J.A. Makawana, X. Zhang, S.C. Teraiya, I. Lin, H.L. Zhu, Design,

synthesis and molecular modeling of pyrazole-quinoline-pyridine hybrids as a new class of antimicrobial and anticancer agents, Eur. J. Med. Chem. 76 (2014) 549-557.

[3] H. Hussain, A. Al-Harrasi, A. Al-Rawahi, I.R. Green, S. Gibbons, Fruitful decade for antileishmanial compounds from 2002 to late 2011, Chem. Rev. 114 (2014) 10369-10428.

[4] P.M. Njogu, K. Chibale, Recent developments in rationally designed multitarget antiprotozoan agents, Curr. Med. Chem. 20 (2013) 1715-1742.

[5] V.V.Kouznetsov, A. Gomez-Barrio, Recent developments in the design and synthesis of hybrid molecules based on aminoquinoline ring and their antiplasmodial evaluation, Eur. J. Med. Chem.44 (2009) 3091-3113.

[6] B. Gryzlo, K. Kulig, Quinoline-a promising fragment in the search for new antimalarials, Mini Rev. Med. Chem. 14 (2014) 332-344.

[7] M.S. Mushtaque, Reemergence of chloroquine analogs as multi targeting antimalarial agents: A review, Eur. J. Med. Chem. 90 (2015) 280-295.

[8] C. Perez-Bolivar, V.A. Montes, P. Anzenbachier, True blue: blue emitting Al^{3+} quinolinolate complexes, Inorg. Chem. 45 (2006) 9610-9612.

[9] H. Wang, W.S. Wang, H.S. Zhang, A spectrofluorimetric method for cysteine and glutathione using the fluorescence system of Zn(II)-8-hydroxyquinoline-5-sulphonic acid complex, Spectrochim. Acta. A 57(12) (2001) 2403-2407.

[10] Y. Wang, S. Astilean, G. Haran, A. Warshawsky, Microenvironmental investigation of polymer bound fluorescent chelator by fluorescence microscopy and optical spectroscopy, Anal. Chem. 73(17) (2001) 4096-4103.

[11] J.B. Mulon, E. Destandau, V. Alain, E. Bardez, How can aluminium(III) generate fluorescence?, J. Inorg. Biochem. 99(90) (2005) 1749-1755.

[12] P. Lienard, J. Gavartin, G. Boccardi, M. Meunier, Predicting drug substances autoxidation, Pharm. Res. 32(1) (2015) 300-310.

[13] G.L. de Souza, L.M. de Oliveira, R.G. Vicari, A. Brown, A DFT investigation on the structural and antioxidant properties of new isolated interglycosidic O-(1→ 3) linkage flavonols, J. Mol. Model., 22(4) (2016) 1-9.

[14] Z. Sroka, B. Żbikowska, J. Hładyszowski, The antiradical activity of some selected flavones and flavonols, Experimental and quantum mechanical study, J. Mol. Model., 21(12) (2015) 1-11.

[15] H. Djeradi, A. Rahmouni, A. Cheriti, Antioxidant activity of flavonoids: a QSAR modeling using Fukui indices descriptors, J. Mol. Model., 20(10) (2014) 1-9.

[16] S. Armaković, S.J. Armaković, S. Koziel, Optoelectronic properties of curved carbon systems, Carbon, 111 (2017) 371-379.

[17] S. Armaković, S.J. Armaković, J.P. Šetrajčić, I.J. Šetrajčić, Active components of frequently used β-blockers from the aspect of computational study, J. Mol. Model., 18(9) (2012) 4491-4501.

[18] S.J. Armaković, S. Armaković, N.L. Finčur, F. Šibul, D. Vione, J.P. Šetrajčić, B. Abramović, Influence of electron acceptors on the kinetics of metoprolol photocatalytic degradation in TiO 2 suspension, A combined experimental and theoretical study, RSC Adv., 5(67) (2015) 54589-54604.

[19] M. Blessy, R.D. Patel, P.N. Prajapati, Y. Agrawal, Development of forced degradation and stability indicating studies of drugs-A review, J. Pharm. Anal., 4(3) (2014) 159-165.

[20] S. Armaković, S.J. Armaković, B.F. Abramović, Theoretical investigation of loratadine reactivity in order to understand its degradation properties: DFT and MD study, J. Mol. Model., 22(10) (2016) 240.

[21] B. Sureshkumar, Y.S. Mary, C.Y. Panicker, S. Suma, S. Armaković, S.J. Armaković, C. Van Alsenoy, B. Narayana, Quinoline derivatives as possible lead compounds for anti-malarial drugs: Spectroscopic, DFT and MD study, Arabian Journal of Chemistry, 2017.

[22] S.J. Armaković, M. Grujić-Brojčin, M. Šćepanović, S. Armaković, A. Golubović, B. Babić, B.F. Abramović, Efficiency of La-doped TiO 2 calcined at different temperatures in photocatalytic degradation of β-blockers, Arabian Journal of Chemistry, 2017, doi.org/10.1016.j.arabjc.2017.01.001.

[23] Y.S. Mary, V. Aswathy, C.Y. Panicker, A. Bielenica, P. Brzózka, O. Savczenko, S. Armaković, S.J. Armaković, C. Van Alsenoy, Spectroscopic, single crystal XRD structure, DFT and molecular dynamics investigation of 1-(3-chloro-4-fluorophenyl)-3-[3-(trifluoromethyl) phenyl] thiourea, RSC Adv., 6(113) (2016) 111997-112015.

[24] Gaussian 09, Revision B.01, M. J. Frisch, G. W. Trucks, H. B. Schlegel, G. E. Scuseria, M. A. Robb, J. R. Cheeseman, G. Scalmani, V. Barone, B. Mennucci, G. A. Petersson, H. Nakatsuji, M. Caricato, X. Li, H. P. Hratchian, A. F. Izmaylov, J. Bloino, G. Zheng, J. L. Sonnenberg, M. Hada, M. Ehara, K. Toyota, R. Fukuda, J. Hasegawa, M. Ishida, T. Nakajima, Y. Honda, O. Kitao, H. Nakai, T. Vreven, J. A. Montgomery, Jr., J. E. Peralta, F. Ogliaro, M. Bearpark, J. J. Heyd, E. Brothers, K. N. Kudin, V. N. Staroverov, T. Keith, R. Kobayashi, J. Normand, K. Raghavachari, A. Rendell, J. C. Burant, S. S. Iyengar, J. Tomasi, M. Cossi, N. Rega, J. M. Millam, M.

Klene, J. E. Knox, J. B. Cross, V. Bakken, C. Adamo, J. Jaramillo, R. Gomperts, R. E. Stratmann, O. Yazyev, A. J. Austin, R. Cammi, C. Pomelli, J. W. Ochterski, R. L. Martin, K. Morokuma, V. G. Zakrzewski, G. A. Voth, P. Salvador, J. J. Dannenberg, S. Dapprich, A. D. Daniels, O. Farkas, J. B. Foresman, J. V. Ortiz, J. Cioslowski, D. J. Fox, Gaussian, Inc., Wallingford CT, 2010.

[25] J.B. Foresman, in: E. Frisch (Ed.), Exploring Chemistry with Electronic Structure Methods: a Guide to Using Gaussian, 1996, Pittsburg, PA.

[26] R. Dennington, T. Keith, J. Millam, GaussView, Version 5, Semichem Inc., Shawnee Mission KS, 2009.

[27] J.M.L. Martin, C. Van Alsenoy, GAR2PED, a Program to Obtain a Potential Energy Distribution from a Gaussian Archive Record, University of Antwerp, Belgium, 2007.

[28] A.D. Bochevarov, E. Harder, T.F. Hughes, J.R. Greenwood, D.A. Braden, D.M. Philipp, D. Rinaldo, M.D. Halls, J. Zhang, R.A. Friesner, Jaguar: A high-performance quantum chemistry software program with strengths in life and materials sciences, Int. J. Quantum Chem., 113(18) (2013) 2110-2142.

[29] D. Shivakumar, J. Williams, Y. Wu, W. Damm, J. Shelley, W. Sherman, Prediction of absolute solvation free energies using molecular dynamics free energy perturbation and the OPLS force field, J. Chem. Theor. Comput., 6(5) (2010) 1509-1519.

[30] Z. Guo, U. Mohanty, J. Noehre, T.K. Sawyer, W. Sherman, G. Krilov, Probing the α-Helical Structural Stability of Stapled p53 Peptides: Molecular Dynamics Simulations and Analysis, Chem. Biol. Drug Design, 75(4) (2010) 348-359.

[31] K.J. Bowers, E. Chow, H. Xu, R.O. Dror, M.P. Eastwood, B.A. Gregersen, J.L. Klepeis, I. Kolossvary, M.A. Moraes, F.D. Sacerdoti. Scalable algorithms for molecular dynamics simulations on commodity clusters. in SC 2006 Conference, Proceedings of the ACM/IEEE. 2006. IEEE.

[32] V.B. Bregović, N. Basarić, K. Mlinarić-Majerski, Anion binding with urea and thiourea derivatives, Coord. Chem. Rev., 295 (2015) 80-124.

[33] A.D. Becke, Density-functional thermochemistry. III. The role of exact exchange, J. Chem. Phys., 98(7) (1993) 5648-5652.

[34] E. Harder, W. Damm, J. Maple, C. Wu, M. Reboul, J.Y. Xiang, L. Wang, D. Lupyan, M.K. Dahlgren, J.L. Knight, OPLS3: a force field providing broad coverage of drug-like small molecules and proteins, J. Chem. Theor. Comput., 12(1) (2015) 281-296.

[35] W.L. Jorgensen, D.S. Maxwell, J. Tirado-Rives, Development and testing of the OPLS all-atom force field on conformational energetics and properties of organic liquids, J. Am. Chem. Soc., 118(45) (1996) 11225-11236.

[36] W.L. Jorgensen, J. Tirado-Rives, The OPLS [optimized potentials for liquid simulations] potential functions for proteins, energy minimizations for crystals of cyclic peptides and crambin, J. Am. Chem. Soc., 110(6) (1988) 1657-1666.

[37] H.J. Berendsen, J.P. Postma, W.F. van Gunsteren, J. Hermans, Interaction models for water in relation to protein hydration, in Intermolecular forces. 1981, Springer. p. 331-342.

[38] Schrödinger Release 2017-3: Maestro, Schrödinger, LLC, New York, NY, 2017. 2017.

[39] G. Varsanyi, Assignments for Vibrational Spectra of Seven Hundred Benzene Derivatives, Wiley, New York, 1974.

[40] Y.S. Mary, C.Y. Panicker, P.L. Anto, M. Sapnakumari, B. Narayana, B.K. Sarojini, Molecular structure, FT-IR, NBO, HOMO and LUMO, MEP and first order hyperpolarizability of (2E)-1-(2,4-dichlorophenyl)-3-(3,4,5-trimethoxyphenyl)prop-2-en-1-one by HF and density functional methods, Spectrochim. Acta 135 (2015) 81-92.

[41] N.P.G. Roeges, A Guide to the Complete Interpretation of Infrared Spectra of Organic Structures, John Wiley and Sons., New York, 1994.

[42] C.Y. Panicker, H.T. Varghese, D. Philip, H.I.S. Nogueira, K. Castkova, Raman, IR and SERS spectra of methyl(2-methyl-4,6-dinitrophenylsulfanyl)ethanoate, Spectrochim. Acta 67 (2007) 1313-1320.

[43] R.T. Ulahannan, C.Y. Panicker, H.T. Varghese, R. Musiol, J. Josef, C. Van Alsenoy, J.A. War, S.K. Srivastava, Molecular Structure, FT-IR, FT-Raman, NBO, HOMO and LUMO, MEP, NLO and molecular docking study of 2-[(E)-2-(2-bromophenyl)-ethenyl]quinoline-6-carboxylic acid, Spectrochim. Acta 151 (2015) 184-197.

[44] N.B. Colthup, L.H. Daly, S.E. Wiberly, Introduction to Infrared and Raman Spectroscopy, Academic Press, New York, 1990.

[45] R.M. Silverstein, G.C. Bassler, T.C. Morril, Spectrometric Identification of Organic Compounds, fifth ed., John Wiley and Sons Inc., Singapore, 1991.

[46] P.K. Ranjith, E.S. Al-Abdullah, F.A.M. Al-Omary, A.A. El-Emam, P.L. Anto, Y.S. Mary, S. Armakovic, S.J. Armakovic, J. Zitko, M. Dolezal, C. Van Alsenoy, FT-IR and FT-Raman characterization and investigation of reactive properties of N-(3-iodo-4-methylphenyl)pyrazine-2-carboxamide by molecular dynamics simulations and DFT calculations, J. Mol. Struct. 1136 (2017) 14-24.

[47] D.A. Zainuri, S. Arshad, N.C. Khalib, I.A. Razak, R.R. Pillai, S.F. Sulaiman,

N.S. Hashim, K.L. Ooi, S. Armakovic, S.J. Armakovic, C.Y. Panicker, Synthesis, XRD crystal structure, spectroscopic characterization (FT-IR, 1H and 13C NMR), DFT studies, chemical reactivity and bond dissociation energy studies using molecular dynamics simulations and evaluation of antimicrobial and antioxidant activities of a novel chalchone derivative, (E)-1-(4-bromophenyl)-3-(4-iodophenyl)prop-2-en-1-one, J. Mol. Struct. 1128 (2017) 520-533.

[48] S.S. Parveen, M.A. Al-Alshaikh, C.Y. Panicker, A.A. El-Emam, B. Narayana, V.V. Saliyan, B.K. Sarojini, C. Van Alsenoy, Vibrational and structural observations and molecular docking study on 1-{3-(4-chlorophenyl)-5-[4-(propan-2-yl)phenyl]-4,5-dihydro-1H-pyrazol-1-yl}-ethanone, J. Mol. Struct. 1112 (2016) 136-146.

[49] K.C. Mariamma, H.T. Varghese, C.Y. Panicker, K. John, J. Vinsova, C. Van Alsenoy, Vibrational spectroscopic investigations and computational study of 5-chloro-2-[4-(trifluoromethyl) phenylcarbamoyl] phenyl acetate, Spectrochim. Acta 112 (2013) 161-168.

[50] D.M. Burland, R.D. Miller, C.A. Walsh, Second order nonlinearity in poled polymer systems, Chem. Rev. 94 (1994) 31-75.

[51] Y.R. Shen, The Principles of Nonlinear Optics, Wiley, New York, 1984.

[52] C. Adant, M. Dupuis, J.L. Bredas, Ab initio study of the nonlinear optical properties of urea, electron correlation and dispersion effects, Int.J. Quantum Chem. 56 (2004) 497-507.

[53] R.T. Ulahannan, C.Y. Panicker, H.T. Varghese, R. Musiol, J. Josef, C. Van Alsenoy, J.A. War, A.A. Al-Saadi, Vibrational spectroscopic and molecular docking study of (2E)-N-(4-chloro-2-oxo-1,2-dihydroquinoline-3-yl]-3-phenylprop-2-enamide, Spectrochim. Acta 151 (2015) 335-349.

[54] R.T. Ulahannan, C.Y. Panicker, H.T. Varghese, R. Musiol, J. Josef, C. Van Alsenoy, J.A.War, T.K. Manojkumar, Vibrational spectroscopic an dmolecular docking study of 2-[(E)-2-phenylethenyl]quinoline-5-carboxylic acid, Spectrochim. Acta 150 (2015) 190-199.

[55] Y.P. Tian, W.T. Yu, C.Y. Zhao, M.H. Jiang, Z.G. Cari, H.K. Fun, Structural characterization and second order nonlinear optical propertie sof zinc halide thiosemicarbazone complexes, Polyhedron 21 (2002) 1217-1222.

[56] K. Fukui, Role of frontier orbitals in chemical reactions, Science 218 (1982) 747-754.

[57] R.G. Parr, R.G. Pearson, Absolute hardness: companion parameter to absolute electronegativity, J. Am. Chem. Soc. 105 (1983) 7512-7516.

[58] J.A. War, K. Jalaja, Y.S. Mary, C.Y. Panicker, S. Armakovic, S.J. Armakovic, S.K.

Srivastava, C. Van Alsenoy, Spectroscopic characterization of 1-[3-(1H-imidazol-1-yl)propyl]-3-phenylthiourea and assessment of reactive and optoelectronic properties employing DFT calculations and molecular dynamics simulations, J. Mol. Struct. 1129 (2017) 72-85.

[59] P. Sjoberg, J.S. Murray, T. Brinck, P. Politzer, Average local ionization energies on the molecular surfaces of aromatic systems as guides to chemical reactivity, Canadian J. Chem., 68(8) (1990) 1440-1443.

[60] J.S. Murray, J.M. Seminario, P. Politzer, P. Sjoberg, Average local ionization energies computed on the surfaces of some strained molecules, Int. J. Quantum Chem., 38(S24) (1990) 645-653.

[61] P. Politzer, F. Abu-Awwad, J.S. Murray, Comparison of density functional and Hartree–Fock average local ionization energies on molecular surfaces, Int.J. Quantum Chem., 69(4) (1998) 607-613.

[62] F.A. Bulat, A. Toro-Labbé, T. Brinck, J.S. Murray, P. Politzer, Quantitative analysis of molecular surfaces: areas, volumes, electrostatic potentials and average local ionization energies, J. Mol. Model., 16(11) (2010) 1679-1691.

[63] P. Politzer, J.S. Murray, F.A. Bulat, Average local ionization energy: a review, J. Mol. Model., 16(11) (2010) 1731-1742.

[64] A. Michalak, F. De Proft, P. Geerlings, R. Nalewajski, Fukui functions from the relaxed

Kohn-Sham orbitals, J. Phys. Chem., A, 103(6) (1999) 762-771

[65] E.D. Glendening, A.E. Reed, J.E. Carpenter, F. Weinhold, NBO Version 3.1, Gaussian Inc., Pittsburgh, PA, 2003.

[66] F. Weinhold, C.R. Landis, Chem. Ed: Res & Pract 2(CERP; special ‘‘structural concepts’’ issue) (2001) 91-104.

[67] M. Szafram, A. Komasa, E.B. Adamska, J. Mol. Struct. 827 (2007) 101-107.

[68] A.E. Reed, L.A. Curtiss, F. Weinhold, Chem. Rev. 88 (1988) 899-926.

[69] S.W. Hovorka, C. Schöneich, Oxidative degradation of pharmaceuticals: theory, mechanisms and inhibition, J. Pharm. Sci., 90(3) (2001) 253-269.

[70] J.S. Wright, H. Shadnia, L.L. Chepelev, Stability of carbon-centered radicals: Effect of functional groups on the energetics of addition of molecular oxygen, J. Comput. Chem., 30(7) (2009) 1016-1026.

[71] G. Gryn'ova, J.L. Hodgson, M.L. Coote, Revising the mechanism of polymer autooxidation, Org. Biomol. Chem., 9(2) (2011) 480-490.

[72] T. Andersson, A. Broo, E. Evertsson, Prediction of Drug Candidates' Sensitivity Toward Autoxidation: Computational Estimation of C-H Dissociation Energies of Carbon-Centered Radicals. J. Pharm. Sci., 103(7) (2014) 1949-1955.

[73] C.H. Kim, P. Leblanc, K.S. Kim, 4-amino-7-chloroquinoline derivatives for treating Parkinson's disease: implications for drug discovery, Expert Opin. Drug Discov., 11(4) (2016) 337–341.

[74] E. Lorenc-Koci, G. Schulze, M. Śmiałowska, A. Kamińska, M. Bajkowska, K. Ossowska, S. Wolfarth, Neurotoxic Factors in Parkinson's Disease and Related Disorders, Springer US 2000.

[75] A. Lagunin, A. Stepanchikova, D. Filimonov, V. Poroikov, PASS: prediction of activity spectra for biologically active substances, Bioinformatics 16 (2000) 747-748.

[76] P. Burkhard, P. Dominici, C. B. Voltattorni, J.N. Jansonius, V.N. Malashkevich, Structural insight into Parkinson's disease treatment from drug-inhibited DOPA decarboxylase, Nature Struct. Biol., 8(2001) 963-967.

[77] A. Barbeau, H. Mars, M.I. Botez, M. Joubert, Levodopa combined with peripheral decarboxylase inhibition in Parkinson's disease, Can. Med. Assoc. J., 106(11) (1972) 1169-1174.

[78] O. Trott, A. J. Olson, AutoDock Vina: Improving the speed and accuracy of docking with a new scoring function, efficient optimization and multithreading, J. Comput. Chem. 31 (2010) 455-461.

[79] B. Kramer, M. Rarey, T. Lengauer, Evaluation of the FlexX incremental construction algorithm for protein ligand docking, Proteins: Struct. Funct.Genet. 37 (1999) 228-241.

[80] F.A.M. Al-Omary, Y.S. Mary, C.Y. Panicker, A.A. El-Emam, I.A. Al-Swaidan, A.A. Al-Saadi, C. Van Alsenoy, Spectroscopic investigations, NO, HOMO-LUMO, NLO analysis and molecular docking of 5-(adamantan-1-yl)-3-anilinomethyl-2,3-dihydro-1,3,4-oxadiazole-2-thione, a potential bioactive agent, J. Mol. Struct. 1096 (2015) 1-14.

Figure captions

Fig.1 FT-IR spectra of 57DC8HQ and 5CL7I8HQ

Fig.2 FT-Raman spectra of 57DC8HQ and 5CL7I8HQ

Fig.3 Optimized molecular geometries of a) 5CL7I8HQ and b) 57DC8HQ

Fig.4 HOMO-LUMO plots of a) 5CL7I8HQ and b) 57DC8HQ

Table 1(a)

Calculated scaled wavenumbers, observed IR, Raman bands and vibrational assignments of 5,7-dichloro-8-hydroxyquinoline (57DC8HQ)

B3LYP/SDD			IR	Raman	Assignments[a]
υ(cm^{-1})	IRI	RA	υ(cm^{-1})	υ(cm^{-1})	-
3463	98.71	61.79	3450	3464	υOH(100)
3090	0.53	75.40	-	-	υCHI(99)
3083	6.83	147.05	3082	-	υCHII(99)
3067	9.22	140.60	-	3070	υCHII(94)
3037	19.25	147.97	3035	3033	υCHII(99)
1591	27.63	34.82	-	1601	υPhI(50), υPhII(23)
1570	17.65	4.10	1575	1569	υPhII(54), δCHII(14), υPhI(10)
1543	12.98	75.42	-	1540	υPhII(45), υPhI(43)
1467	63.63	14.65	1467	1465	δCHII(15), υPhII(46), υPhI(18)
1432	115.74	1.61	-	1435	δCHII(12), υPhI(57), υPhII(22)
1385	139.90	126.31	-	1388	δOH(38), υPhI(39)
1368	26.00	25.59	1370	1371	δCHII(12), δCHI(16), υPhI(45)
1348	18.74	8.91	-	1344	δCHII(12), υPhII(41), υPhI(18)
1315	148.26	120.14	1322	1318	υPhII(61), δOH(15)
1245	48.16	14.18	-	1248	δCHII(18), υCO(42)
1212	22.33	8.95	1215	1215	υPhI(12), δCHI(55), υPhII(11)
1188	64.99	12.06	1190	-	υPhI(17), δCHII(56), δOH(12)

1178	47.84	3.17	-	1176	υPhI(31), υPhII(23), δCHI(19)
1121	19.03	10.37	-	1128	δCHII(43), υPhII(22)
1067	15.10	1.12	1060	1070	υCO(13), δCHII(44)
1023	9.01	19.73	-	1022	υPhI(62), δCHII(12)
957	0.29	0.63	957	958	γCHII(89)
925	0.01	0.18	-	928	γCHII(90)
924	58.68	2.36	-	918	δPhI(32), υCCl(19), δPhII(15)
858	23.02	0.84	860	-	δPhII(39), υCCl(19), υPhI(10)
849	17.22	0.34	-	851	γCHI(84)
782	27.52	0.28	784	770	γCHII(71), τPhII(13)
764	13.39	0.33	-	770	τPhI(34), τPhII(30), γCO(15)
713	39.94	0.51	716	716	υCCl(49), δPhI(16), δPhII(20)
705	23.00	29.39	-	703	δPhI(25), δPhII(15), υCCl(50)
653	12.93	0.69	655	651	γCO(12), τPhII(10), τPhI(15), υCCl(36)
607	13.86	0.27	609	610	δPhII(50), δCO(17), δCCl(17)
592	88.75	0.47	-	-	τOH(62) , γCCl(10), τPhI(10)
582	17.57	0.57	585	-	τPhI(32), γCCl(23), τOH(12), τPhII(13)
564	8.32	3.48	-	565	δPhII(42), δCCl(21)
491	0.09	0.05	505	494	τPhII(30), γCCl(22), τPhI(31)
487	0.37	6.63	478	482	δPhI(56), δPhII(19)
420	0.98	1.42	-	419	τPhII(65), τPhI(10)
368	4.57	15.67	-	365	δPhI(35), δPhII(39)
346	0.06	0.03	-	-	γCCl(47), γCO(21),

					τPhII(19)
344	2.13	5.80	-	-	δPhI(56), υCCl(20)
282	6.44	0.01	-	280	δCO(50), δPhI(19)
234	1.33	0.15	-	232	τPhII(58), τPhI(20)
210	1.55	2.28	-	-	δCCl(63)
183	0.12	2.73	-	185	δCCl(87)
146	0.22	0.62	-	-	τPhI(55), τPhII(28)
130	0.01	1.40	-	-	γCCl(49), τPhII(22)
79	0.92	0.73	-	81	τPhI(72), τPhII(16)

Table 1(b)

Calculated scaled wavenumbers, observed IR, Raman bands and vibrational assignments of 5-chloro-7-iodo-8-hydroxy quinoline (5CL7I8HQ)

B3LYP/SDD			IR	Raman	Assignments[a]
υ(cm^{-1})	IRI	RA	υ(cm^{-1})	υ(cm^{-1})	-
3474	113.64	73.58	3445	-	υOH(100)
3124	16.96	231.01	-	3127	υCHII(99)
3119	0.89	47.50	-	-	υCHI(99)
3104	6.60	85.39	-	3099	υCHII(100)
3088	10.86	96.09	3085	3074	υCHII(96)
1593	15.42	57.13	1602	1601	υPhI(49), υPhII(14)
1561	25.18	4.82	1565	1565	υIIPh (45),υPhI(16)
1536	22.26	78.60	-	-	υPhI(44), υPhII(42)
1458	57.22	8.30	1458	1460	δCHII(17), υPhII(57), υPhI(13)
1423	60.44	9.12	-	-	δCHII(12), υPhI(56), υPhII(11)
1390	46.56	310.16	1393	1390	υPhI(65)
1365	33.28	8.97	1369	-	δOH(41), δCHI(19), υPhI(19)

1351	42.76	2.26	-	1349	δCHII(12),υPhII(55)
1304	166.57	15.47	1315	1307	υPhII(44), υPhI(44)
1237	56.56	4.24	1233	-	υCO(43), δCHI(11), δCHII(21)
1219	22.68	22.65	1210	1223	υPhI(28), υCO(14), υPhII(23)
1187	53.34	0.84	-	-	δCHI(52), υPhI(13), υPhII(12)
1163	104.31	11.89	-	1168	δOH(12), δCHII(50), υPhI(10)
1120	38.96	13.31	1125	1125	δCHII(48), υPhI(12), υPhII(19)
1056	12.53	3.43	1049	1050	δCHII(57), υPhII(22)
1016	8.66	24.31	-	-	υPhI(59), δPhI(14)
1000	0.52	1.30	-	-	γCHII(88)
952	0.41	0.22	954	949	γCHII(87)
900	49.23	3.21	-	905	δPhII(23), δPhI 29), υCCl(16), υPhII(10)
892	13.26	3.45	885	-	γCHI(83)
833	36.08	1.93	835	835	τPhII (15),τPhI(11), γCHII(64)
827	15.13	1.63	-	-	δPhII(31), δPhI(21), υPhI(11)
797	20.22	1.06	793	803	τPhI(29), τPhII(20), γCHII(23), γCO(14)
695	23.36	36.76	705	-	δPhII(16), δPhI(20),υPhI(19)
665	55.19	3.32	-	-	γCO(28),τPhII(24),τPhI(27)
657	116.09	1.59	-	-	τOH(88)
654	32.83	0.79	650	654	υCCl(35),δPhI(17), υCI(13), δPhII(12)
602	1.61	0.81	607	608	γCCl(23), τPhI(33), τPhII(19), γCO(11)
591	11.27	1.71	593	-	δPhII(53),δCO(18)

542	15.07	5.38	-	-	δPhII(37),δCCl(18)
493	1.69	1.63	495	495	τPhII(32),τPhI(34),γCI(18)
486	0.78	5.71	-	484	δPhI(58), δPhII(19)
429	2.76	3.17	-	426	τPhII(64),τPhI(10)
346	0.87	1.30	-	-	γCCl(27), γCO(21), γCI(19), τPhII(18)
345	3.03	12.74	-	340	υCI(37), δPhI(11), τPhII(17)
284	8.45	3.86	-	-	δCO(47),δCCl(12)
226	1.24	1.08	-	230	τPhII(63), γCI(10)
219	2.93	3.65	-	216	δPhI(24), δCCl(17)
172	0.81	5.15	-	172	δCCl(41), υCI(33)
150	0.19	0.50	-	149	τPhI(57), τPhII(11)
121	0.01	1.54	-	-	γCCl(30), γCI(21), τPhII(15), τPhI(13)
120	0.66	2.62	-	115	δCI(78), δCCl(11)
67	2.26	1.65	-	-	τPhI(60), γCI(13), τPhII(10)

[a]υ-stretching; δ-in-plane deformation; γ-out-of-plane deformation; τ-torsion; , PhI-C1-C2-C3-C4-C5-C6; PhII-C4-C5-C10-C9-C8-N7; IR_I-IR intensity(KM/Mole) ; RA-Raman activity(Å^4/amu).

Table 2

PASS prediction for the activity spectrum of the title compounds

Pa represents probability to be active and Pi represents probability to be inactive.

Table 2(a)

5,7-dichloro-8-hydroxyquinoline (57DC8HQ)

Pa	Pi	Activity
0.964	0.002	Antiseborrheic
0.911	0.003	Dehydro-L-gulonate decarboxylase inhibitor
0.894	0.003	Glutathione thiolesterase inhibitor
0.892	0.004	Glycosylphosphatidylinositol phospholipase D inhibitor
0.879	0.003	Phthalate 4.5-dioxygenase inhibitor
0.868	0.004	Alkane 1-monooxygenase inhibitor
0.861	0.002	Biphenyl-2.3-diol 1.2-dioxygenase inhibitor
0.860	0.003	2-Hydroxyquinoline 8-monooxygenase inhibitor
0.857	0.002	Antiprotozoal (Amoeba)
0.855	0.003	Corticosteroid side-chain-isomerase inhibitor
0.845	0.002	Hydroxylamine oxidase inhibitor
0.844	0.004	Nitrate reductase (cytochrome) inhibitor
0.835	0.004	Creatininase inhibitor
0.834	0.004	Antiseptic
0.827	0.004	Amine dehydrogenase inhibitor
0.826	0.003	Cis-1.2-dihydro-1.2-dihydroxynaphthalene dehydrogenase inhibitor
0.823	0.010	Glucose oxidase inhibitor
0.817	0.006	CarboxypeptidaseTaq inhibitor
0.813	0.002	Nicotine dehydrogenase inhibitor
0.808	0.010	Arylacetonitrilase inhibitor

Table 2(b)

5-chloro-7-iodo-8-hydroxy quinoline (5CL7I8HQ)

Pa	Pi	Activity
0.965	0.002	Antiprotozoal (Amoeba)
0.919	0.004	Antiinfective
0.898	0.004	Antiseborrheic

0.872	0.004	Dehydro-L-gulonate decarboxylase inhibitor
0.847	0.004	Glutathione thiolesterase inhibitor
0.846	0.006	Glycosylphosphatidylinositol phospholipase D inhibitor
0.840	0.004	Antiseptic
0.829	0.004	Phthalate 4.5-dioxygenase inhibitor
0.810	0.005	Alkane 1-monooxygenase inhibitor
0.803	0.003	Nitrite reductase [NAD(P)H] inhibitor
0.796	0.005	2-Hydroxyquinoline 8-monooxygenase inhibitor
0.786	0.004	Corticosteroid side-chain-isomerase inhibitor
0.785	0.003	Antiprotozoal
0.781	0.003	Hydroxylamine oxidase inhibitor
0.776	0.003	Hydroxylamine reductase (NADH) inhibitor
0.803	0.032	Ubiquinol-cytochrome-c reductase inhibitor
0.753	0.004	Cis-1.2-dihydro-1.2-dihydroxynaphthalene dehydrogenase inhibitor

Table 3

The binding affinity values of different poses of the title compounds predicted by AutodockVina.

Table 3(a)

5,7-dichloro-8-hydroxyquinoline (57DC8HQ)

Mode	Affinity (kcal/mol)	Distance from best mode (Å)	
-	-	RMSD l.b.	RMSD u.b.
1	-6.0	0.000	0.000
2	-4.9	10.876	11.296
3	-4.9	22.723	23.599
4	-4.8	3.471	5.016
5	-4.8	2.646	2.865
6	-4.7	23.121	23.918
7	-4.7	2.505	2.655
8	-4.7	5.344	5.730
9	-4.6	22.067	22.755

Table 3(b)

5-chloro-7-iodo-8-hydroxy quinoline (5CL7I8HQ)

1	-5.1	0.000	0.000
2	-5.0	4.094	5.297
3	-4.9	3.679	4.576
4	-4.8	3.488	4.822
5	-4.8	2.585	3.835
6	-4.8	2.845	3.226
7	-4.8	24.392	25.911
8	-4.7	2.375	2.513
9	-4.7	3.903	5.601

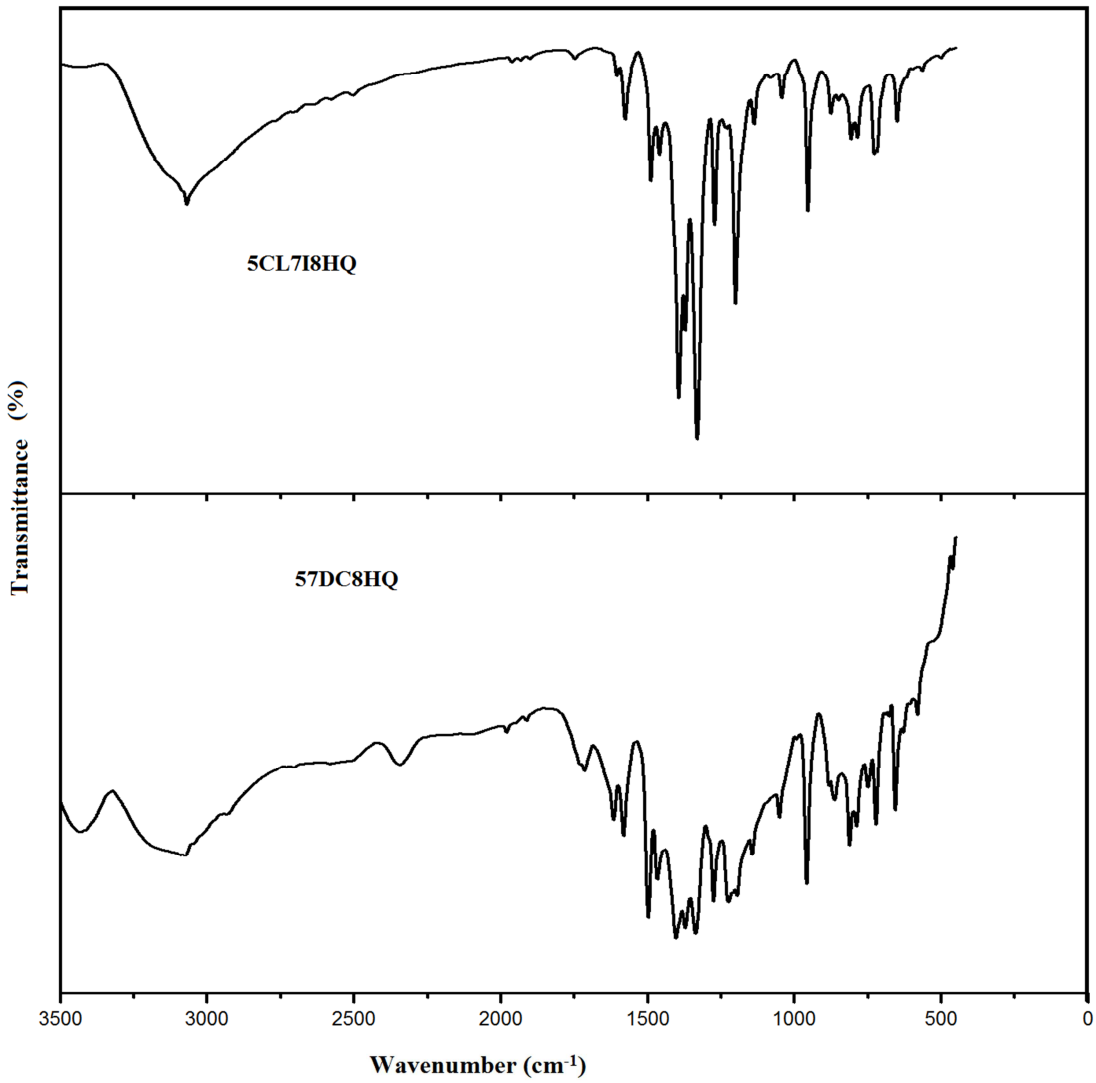
5CL7I8HQ
57DC8HQ
Transmittance (%)
3500
3000
2500
2000
1500
1000
500
0
Wavenumber (cm-1)

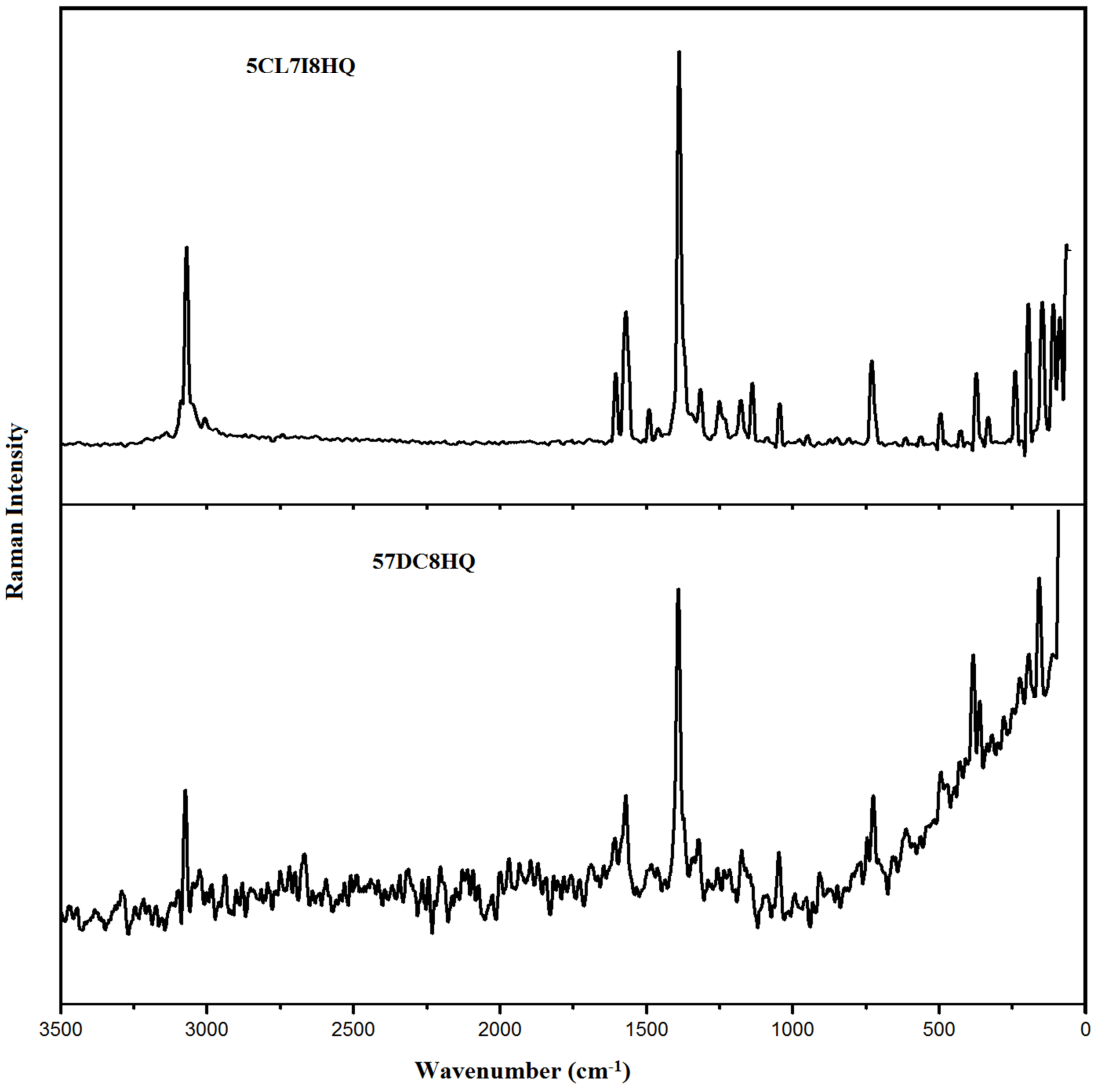
5CL7I8HQ
57DC8HQ
Raman Intensity
3500
3000
2500
2000
1500
1000
500
0
Wavenumber (cm-1)

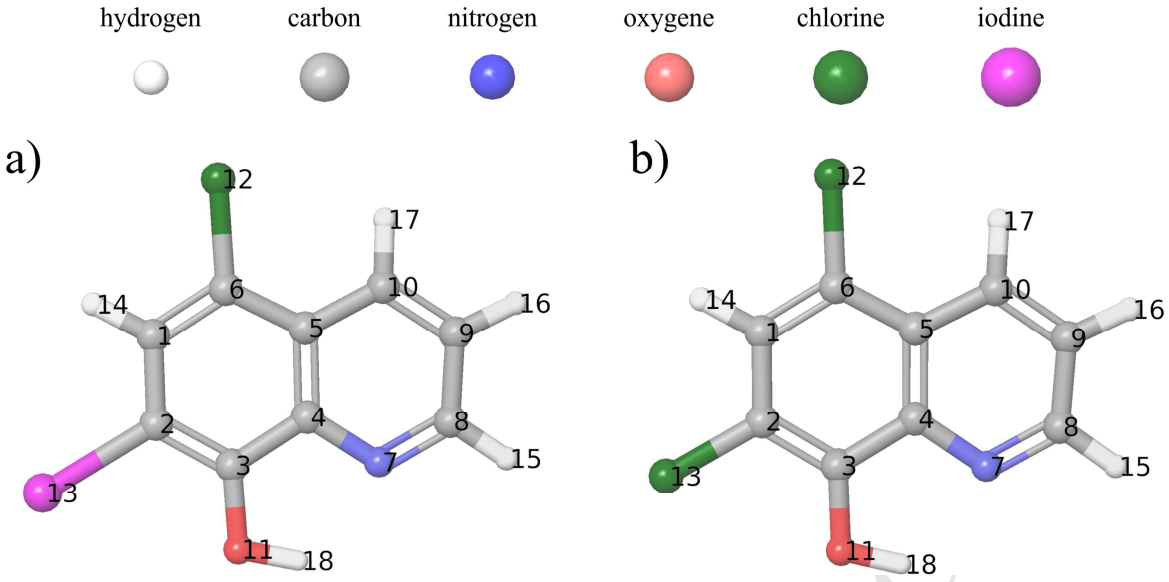

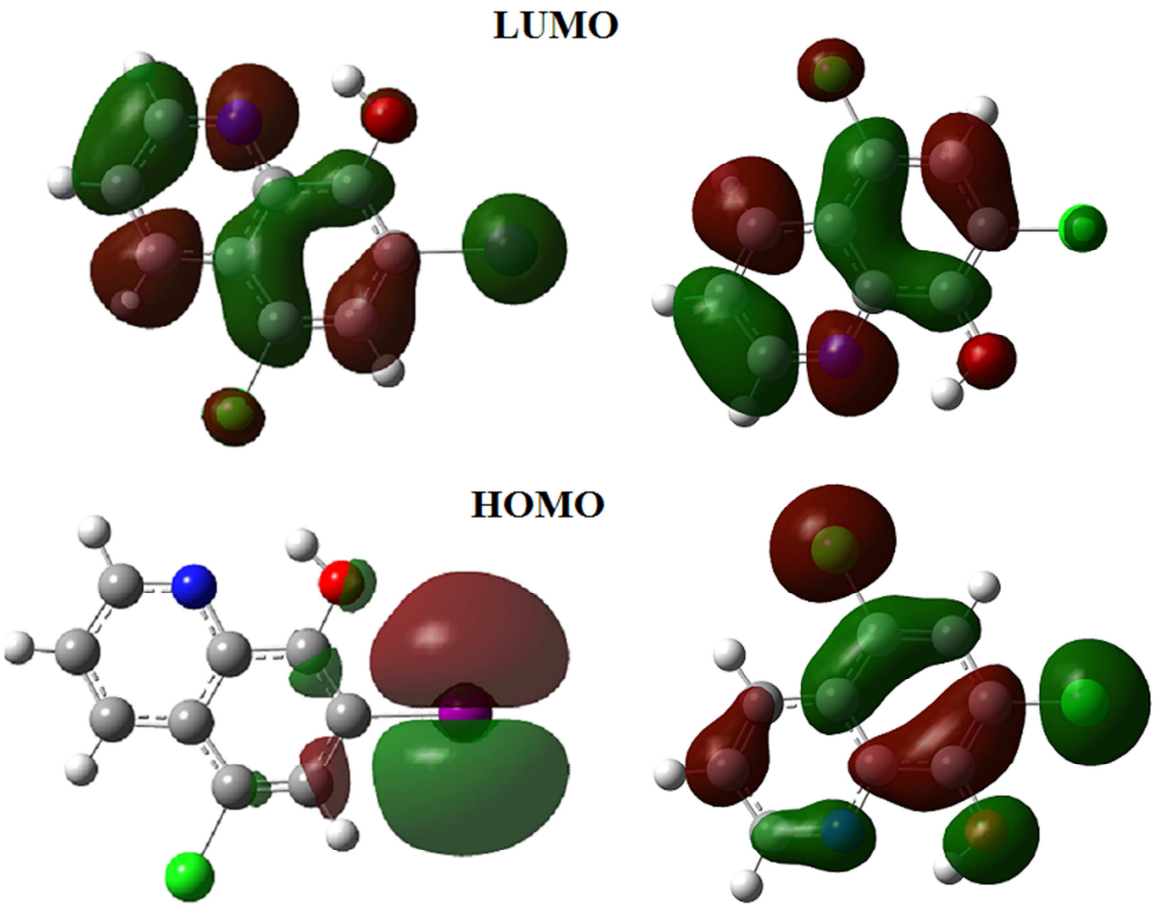

a) 5CL7I8HQ b) 57DC8HQ

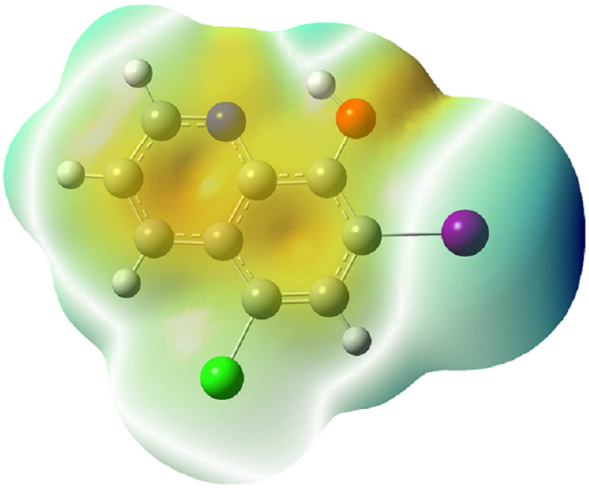

a)5CL7I8HQ

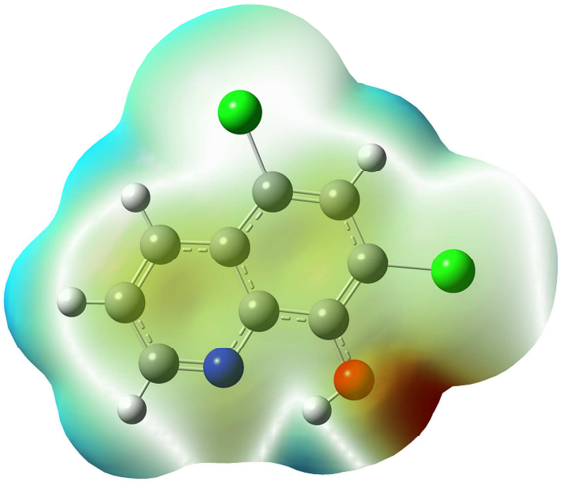

b)57DC8HQ

a)

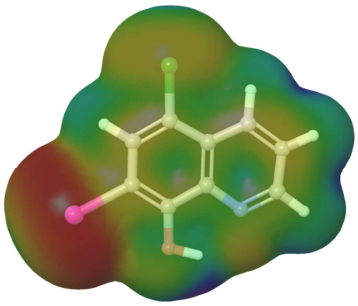

182.48 ALIE [kcal/mol] 382.43

b)

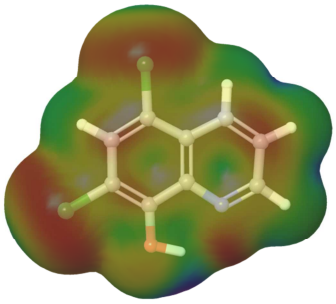

218.53 ALIE [kcal/mol] 383.32

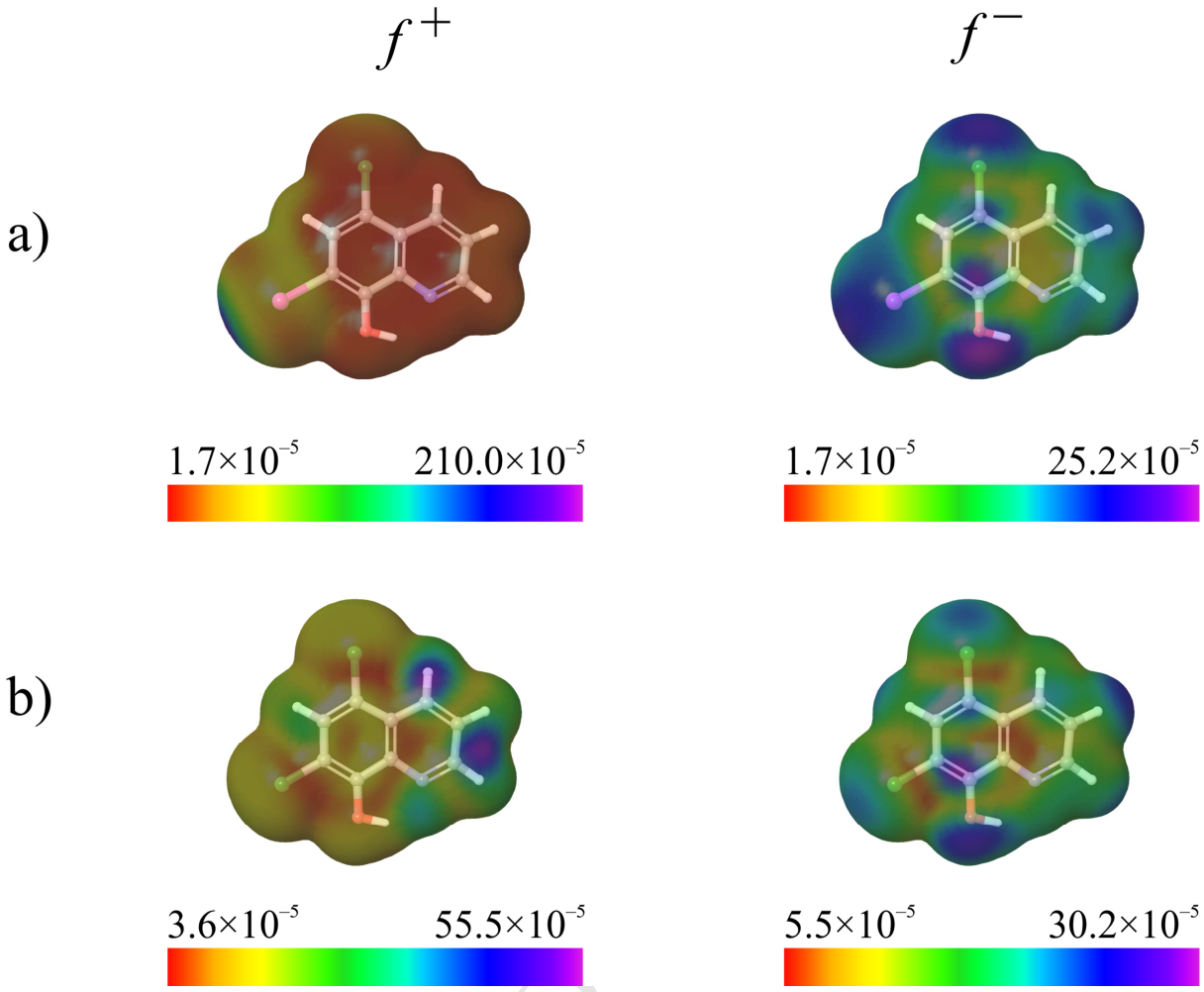
f^+
f^-
a)
1.7×10^{-5}
210.0×10^{-5}
1.7×10^{-5}
25.2×10^{-5}
b)
3.6×10^{-5}
55.5×10^{-5}
5.5×10^{-5}
30.2×10^{-5}

a)

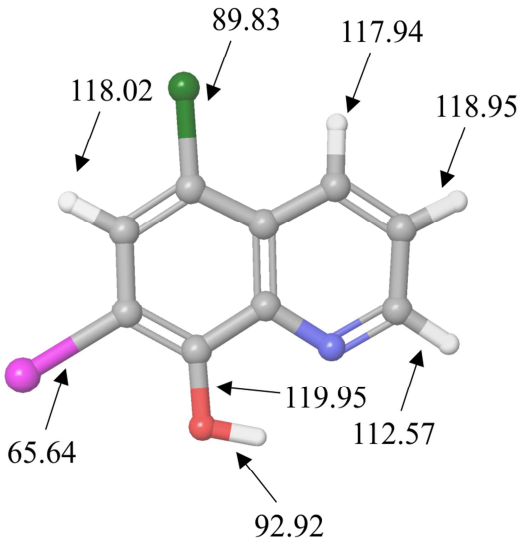

b)

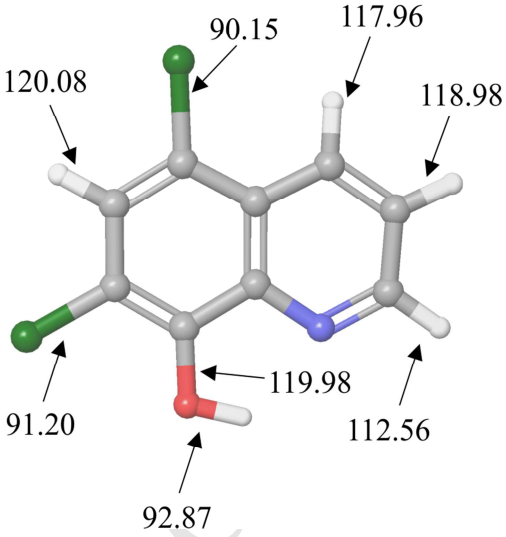

a)

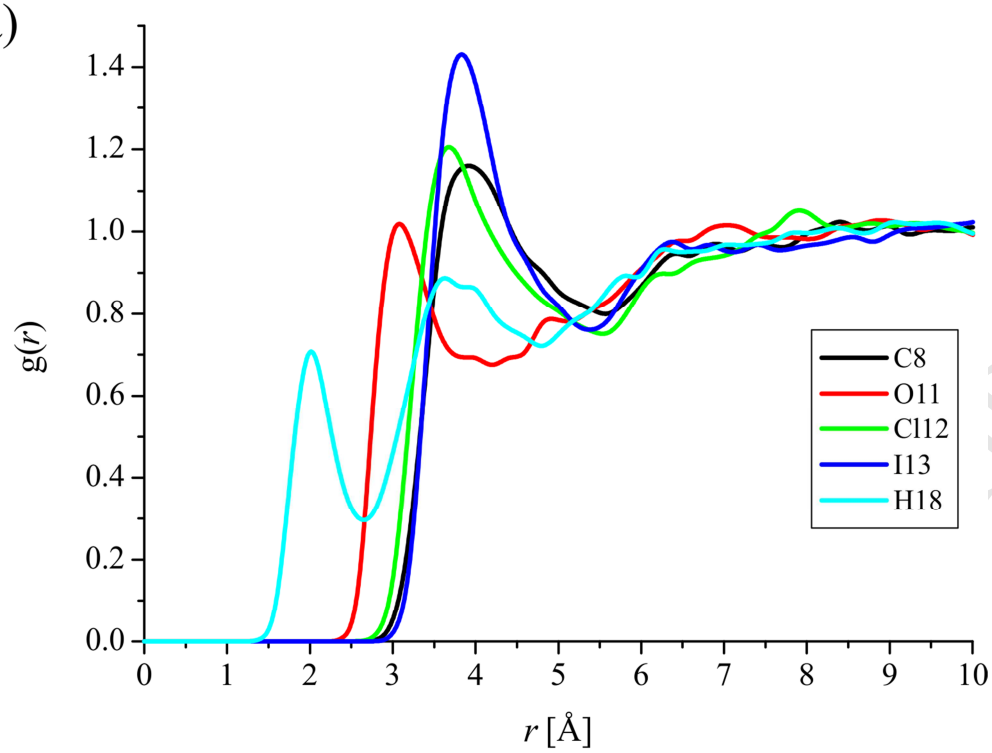

b)

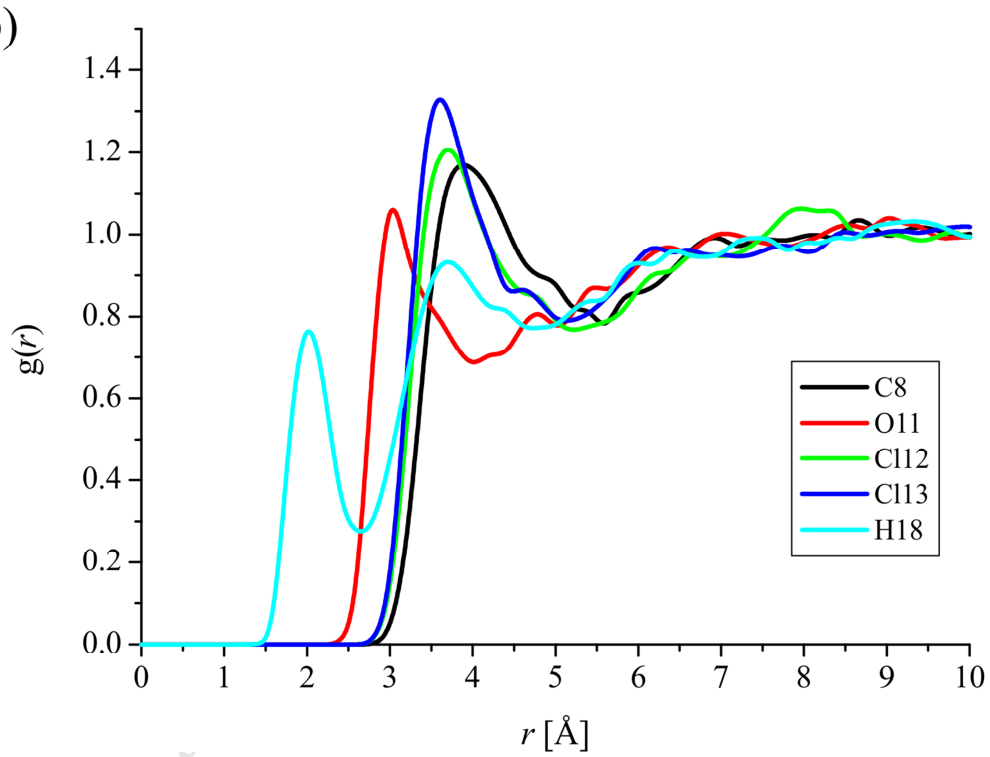

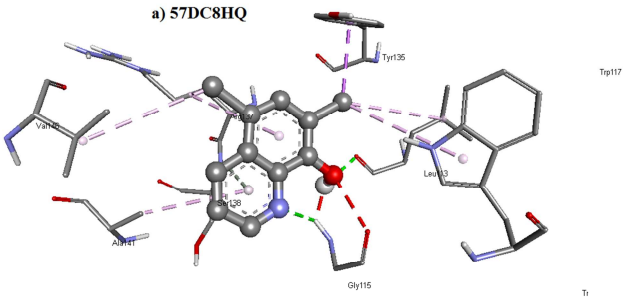

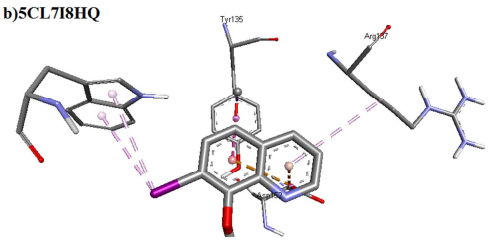

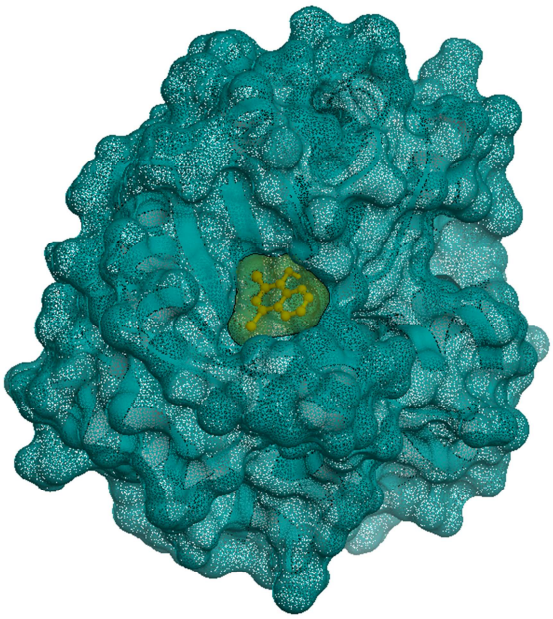

57DC8HQ

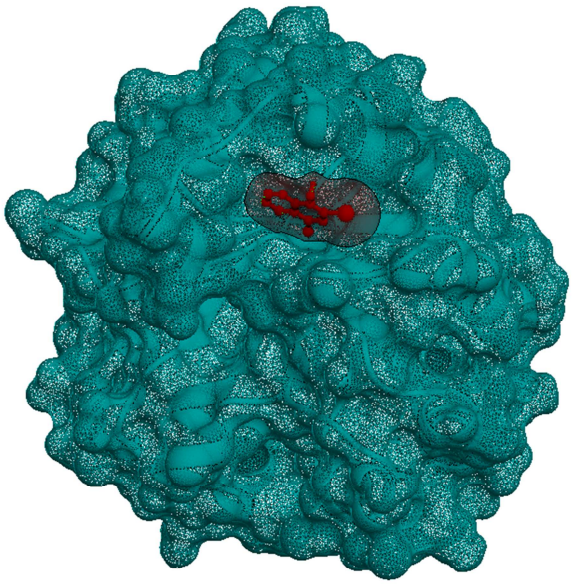

5CL7I8HQ

Highlights

* FT-IR and FT-Raman spectra were measured
* Studied NLO behavior, MEP and NBO analysis
* ALI, BDE, RDF have been discussed in detail
* Molecular docking studies have been reported.